

RIS-Aided Monitoring With Cooperative Jamming: Design and Performance Analysis

Shuying Lin, Yulong Zou, *Senior Member, IEEE*, Zhiyang Li, Eduard E. Bahingayi, and Le-Nam Tran, *Senior Member, IEEE*

Abstract—Exploiting the potential of physical-layer signals to monitor malicious users, we investigate a reconfigurable intelligent surface (RIS) aided wireless surveillance system. In this system, a monitor not only receives signal from suspicious transmitter via a RIS-enhanced legitimate surveillance (LS) link but also simultaneously takes control of multiple jammers to degrade the quality of received suspicious signal. Under this setup, to enhance monitoring performance requires improvements of both the received signal quality at the monitor and the cooperative jamming (CJ). Considering that the surveillance system is aided by one RIS, whose phase shift optimization involves both channel state information (CSI) of the LS and CJ links, we utilize partial CSI to alleviate the CSI acquisition burden in our design. We propose two RIS-aided monitoring schemes with optimal jammer selection (OJS), which are differentiated by the knowledge of the involving links for the phase shift design of RIS. Specifically, the proposed schemes are named the RIS-aided monitoring with the CSI of LS link and an optimal selected jammer (RISLO) and RIS-aided monitoring with the CSI of CJ link and an optimal selected jammer (RISCO), and their closed-form expressions of surveillance success probability (SSP) are derived, respectively. Furthermore, we consider RIS-aided monitoring schemes with random jammer selection as corresponding benchmarks. Thereafter, we analyze special cases where the jammers are using power control to avoid being found, making it appears like passive monitoring. Also, the effect of RIS is highlighted by considering asymptotically large number of RIS elements. Numerical results verify that the proposed OJS strategy further enhances the RIS-aided monitoring performance compared with non-jammer-selection RISLR and RISCRC schemes, where the superiority comes at the cost of CSI knowledge and becomes marginal in the region of high jamming power. In addition, the RISLO shows surveillance performance advantage over RISCO when the suspicious power is low or when the number of RIS elements is large.

Index Terms—Monitoring, cooperative jamming, reconfigurable intelligent surface, surveillance success probability, jammer selection.

This work was supported in part by the National Natural Science Foundation of China (Grant Nos. 62271268 and 62071253), in part by the Jiangsu Provincial Key Research and Development Program (Grant No. BE2022800), in part by the Jiangsu Provincial 333 Talent Project, in part by research grants from Science Foundation Ireland (SFI) under Grant Nos. 22/US/3847 and 17/CDA/4786, and in part by China Scholarship Council (CSC). (*Corresponding author: Yulong Zou.*)

S. Lin and Y. Zou are with the School of Telecommunications and Information Engineering, Nanjing University of Posts and Telecommunications, Nanjing, China.

Z. Li is with the School of Electronics and Information Engineering, Harbin Institute of Technology, Harbin, China.

Eduard E. Bahingayi and L.-N. Tran are with the School of Electrical and Electronic Engineering, University College Dublin, D04 V1W8, Ireland.

I. INTRODUCTION

Wireless connectivity has become a cornerstone in our modern society but it also raises serious concerns over information privacy. Thus, numerous research endeavors have been made to enhance wireless security [1], [2], [3]. In this context, the rise of ad-hoc or mesh-type communication technologies, such as device-to-device (D2D) communications, presents new vulnerabilities. These technologies can be leveraged by malicious users to jeopardize public safety, commit crimes, coordinate terrorist activities, or illegally transmit confidential trade information [4]. Addressing these threats calls for the implementation of legitimate surveillance as a critical component of wireless communication security. For example, the National Security Agency of the United States launched the Terrorist Surveillance Program in 2006 to proactively monitor and counter potential threats [5]. However, the rapidly increasing number of malicious wireless devices over the past decade still poses growing concerns over security threats. This highlights the need for a paradigm shift from preventing conventional eavesdropping attacks to adopting legitimate surveillance as a critical tool [6].

Physical-layer surveillance (i.e., monitoring) takes advantage of the broadcast nature of wireless propagation [2]. As an extension of secrecy rate, outage probability, and intercept probability, etc., defined for physical layer security (PLS) performance analysis [11], similar fundamental metrics have been adapted to evaluate the performance of wireless surveillance strategies. Specifically, the authors of [6] introduced the average eavesdropping rate as a performance metric for monitoring, emphasizing that the monitor operates effectively only when its achievable rate for intercepting suspicious signals is greater than the suspicious communication rate. Also, since the monitor overhears the suspicious signals for surveillance purposes, the data rate of this received signal can be regarded as the monitoring rate. Furthermore, similar to the secrecy rate, which is the difference between the data rates of a legitimate user and an eavesdropper, the relative monitoring rate (RMR) is defined as the difference between the data rates of the legitimate surveillance channel and the suspicious channel [10]. The probability of a successful surveillance event, known as the surveillance success probability (SSP) [13], is defined as the probability that the RMR is larger than a target threshold. For example, the authors of [18] studied jamming power allocation to maximize the RMR under an average transmit power constraint. To solve their considered problems, both the bisection search and the Lagrange duality method were

applied.

A legitimate monitor either silently receives suspicious signals or performs proactive eavesdropping via spoofing relaying [7] or cooperative jamming (CJ) [9]. The technique of CJ have been widely investigated to degrade the received signal of eavesdroppers [jiangxiaointelligent, #li_jsrs]. Specifically, the authors of [jiangxiaointelligent] proposed a threshold-based selection to validate friendly jamming, and formulated a subset of jammers whose channel quality is good enough to be chosen. In fact, the proactive monitoring is inspired by conventional PLS methods to simultaneously combat eavesdropping and jamming attacks [8]. When gains of the legitimate surveillance channel are significantly weaker than those of the suspicious channel, passive monitoring becomes inefficient because of its inability to decode suspicious messages. For such situations, proactive monitoring via cooperative jamming is emerging as a more competitive candidate than passive monitoring. Specifically, the authors of [16] studied two-phase relay-aided suspicious communication system and proposed two strategies, namely “passive eavesdropping first” and “jamming first” to maximize the sum eavesdropping rate subject to finite transmit power of the monitor.

While wireless surveillance has been regarded as a promising approach to monitor suspicious communications, its performance is still restricted by uncontrollable radio environments in practice [4]. To this end, reconfigurable intelligent surfaces (RISs), with their unprecedented capability of shaping wireless propagation environments, emerge as an effective solution when integrated with wireless surveillance. Thus, extensive efforts have been devoted to RIS-aided wireless surveillance. Specifically, the authors of [28] considered passive monitoring assisted by a RIS, where signals from a suspicious transmitter to a suspicious user was also intercepted via a RIS-aided legitimate link. In [25], a full-duplex legitimate monitor was studied with proactive eavesdropping by means of CJ, where the monitoring rate maximization problem for three RIS deployment strategies was formulated. Then, a near-optimal performance was achieved by jointly optimizing the receive and jamming beamforming vectors at the legitimate monitor and the reflection coefficients at the RIS. The authors of [24] investigated a robust design for a RIS-aided wireless information surveillance system with bounded channel errors. In [24], by jointly optimizing the RIS phase shifts and receiver beamformer, the worst-case information monitoring rate was maximized to improve surveillance performance. In [26], a scheme named RIS-assisted cooperative jamming was proposed to combat suspicious communications. However, the jammer was unable to obtain information from suspicious communications in [26].

Extensive research efforts have been devoted to performance analysis of monitoring suspicious communications via CJ, as can be seen from the aforementioned works. However, few studies have explored RIS-aided monitoring with opportunistic selection among multiple jammers. To address this gap, in this paper, we study a RIS-aided wireless surveillance system assisted by multiple jammers. The main contributions of this paper are summarized as follows. First, we present two novel RIS-aided monitoring schemes with optimal jammer selection,

which are differentiated by the knowledge of the involving links for the phase shift design of RIS. In most of existing works, all cascade links are perfectly known by the central controller, e.g., the monitor, and the optimal phase shift is formulated by an objective function related different links. To seek a tradeoff between this phase shift optimization and more practically applicable random phase shifts, this paper utilizes partial channel state information (CSI) to compute phase shift values. In the first scheme, referred to as RISLO, the phase shift is designed according to the knowledge of the legitimate surveillance (LS) link. In the second one, called RISCO, the knowledge of CJ link is employed instead. These two schemes are compared with two corresponding benchmark schemes random jammer selection (RJS), referred to as RISLR and RISCR, both of which are also firstly proposed in this work. Furthermore, we derive closed-form SSP expressions of the proposed schemes and carry out in-depth asymptotic analysis, based on which some interesting observations are obtained. Specifically, the RISLO and RISLR show superiorities over the RISCO and RISCR, respectively, because the CSI database for phase shift design and jammer selection includes both knowledges of LS and CJ links. This indicates that how well the monitoring schemes behave depends on the utilization level of CSI of the overall system, showing the existence of a tradeoff between interaction/computation overhead and performance limitation. Also, we discuss the performance ceilings when the jamming power becomes higher. In this case, the CSI requirement is alleviated, accompanied with more power consumption. Moreover, we explore an useful case that the jammers become almost passive with an asymptotically large number of RIS elements. The asymptotic analysis has theoretically proved that the RISLO outperforms the RISCO, unless the monitoring channels are much better than the suspicious channels.

The rest of the paper is organized as follows. Section II describes the wireless surveillance system model. In Section III, we derive closed-form SSP expressions of proposed schemes for different cases of RIS phase shifts and jammer selection. Some asymptotic analysis is further presented in Section IV. Numerical results are presented in Section V. Finally, Section VI concludes the paper.

Notations: Boldface lowercase letters and boldface uppercase ones are used for vectors and matrices, respectively. For a complex variable, $|\cdot|$ denotes its absolute value. For a complex vector, $(\cdot)^T$ and $(\cdot)^H$ denote its respective transpose and Hermitian transpose. Also, \mathbb{C}^N and $\mathbb{C}^{M \times N}$ represent the complex-valued space of N -dimensional vectors and the complex-valued space of M -by- N matrices, respectively. Notations \sim , and $\stackrel{\Delta}{=}$ stand for “distributed as” and “to be defined as”, respectively. Besides, $n!$ represents the factorial of a non-negative number n , $\text{diag}(\mathbf{a})$ denotes a diagonal matrix with its diagonal elements given by \mathbf{a} , $\arg(\cdot)$ represents the phase of a complex number, i.e., $a = |a|\arg(a)$, $E(\cdot)$ and $\text{Var}(\cdot)$ represent the statistical expectation and variance operators, respectively, $C_{p,q}^{m,n}(\cdot)$ is the Meijer G-function [26, Eq. (9.301)], and $\Gamma(\cdot, \cdot)$ represents the upper incomplete gamma function, among which a special case is the gamma function, noted as

$\Gamma(0, \cdot) = \Gamma(\cdot)$, where exists $\Gamma(n+1) = n!$ for a non-negative number n . Additionally, $\binom{N}{n}$ is the number of possible cases to pick n elements from a set with N elements.

II. SYSTEM MODEL

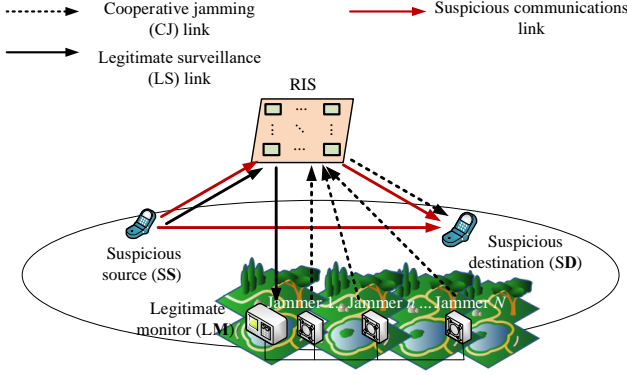


Fig. 1. An RIS-aided wireless monitoring system assisted by multiple jammers.

A. RIS-Aided Monitoring System

As illustrated in Fig. 1, we consider a wireless monitoring system consisting of a pair of suspicious source and destination (SS-SD), a legitimate monitor (LM) including multiple distributed jammers, and a RIS with L co-located reflecting elements.¹ The sets of RIS elements and jammers are denoted as $\mathcal{L} \triangleq \{1, 2, \dots, L\}$ and $\mathcal{N} \triangleq \{1, 2, \dots, N\}$, respectively. One jammer is opportunistically selected to perform cooperative jamming (CJ) to suspicious nodes based on a specific selection criterion. When the SS transmits a signal to the SD at a power of P_s , the LM can overhear the signal intended for the SD. The received signal at the LM is written as

$$y_M = \sqrt{P_s}(\mathbf{h}_{RM}^H \Theta \mathbf{h}_{SR})x_s + n_M, \quad (1)$$

where x_s is the normalized symbol, i.e., $E(|x_s|^2) = 1$, $\mathbf{h}_{RM}^H \in \mathbb{C}^{1 \times L}$, and $\mathbf{h}_{SR} \in \mathbb{C}^{L \times 1}$ are channel coefficients of RIS-M and SS-RIS transmissions, respectively, Θ_n is the reflection coefficient diagonal matrix defined as

$\Theta = \text{diag}([e^{-j\phi_1}, \dots, e^{-j\phi_l}, \dots, e^{-j\phi_L}])$, where $\phi_l \in [0, 2\pi)$ denotes the phase shift for each element $l \in \mathcal{L}$, and n_M is the additive white Gaussian noise (AWGN) with a zero mean and a variance of N_0 . In the considered system model, it is assumed that the direct links between the LM, the jammers and suspicious nodes are severely blocked. Consequently, the LM and the jammers need to rely on the RIS to monitor the suspicious nodes.

When the LM detects the presence of active suspicious nodes, a jammer $n \in \mathcal{N}$ is selected to send a jamming signal x_J deliberately at a power of P_J (which is not the case for passive monitoring) to decrease the signal-to-interference-plus-noise

ratio (SINR) at the SD. Thus, the received signal at the SD is given by

$$y_{D,n} = \sqrt{P_s}(h_{SD} + \mathbf{h}_{RD}^H \Theta \mathbf{h}_{SR})x_s + \sqrt{P_J}(\mathbf{h}_{RD}^H \Theta \mathbf{h}_{nR})x_J + n_D, \quad (2)$$

where h_{SD} , $\mathbf{h}_{RD}^H \in \mathbb{C}^{1 \times L}$, $\mathbf{h}_{SR} \in \mathbb{C}^{L \times 1}$, and $\mathbf{h}_{nR} \in \mathbb{C}^{L \times 1}$ are channel coefficients of SS-SD, RIS-SD, SS-RIS transmission, and of the link from the n -th jammer to the RIS, respectively, $n \in \mathcal{N}$, and n_D is the AWGN with a zero mean and a variance of N_0 at the SD. We note that, with active jamming coming into play, the signal model at the LM in (1) should include an interference due to the RIS reflection of the jamming signal x_J . However, since the jamming signal is already known by the LM, the reflected interference can be effectively suppressed to a negligible level if the LM can estimate the channel of the composite LM-RIS links [12]. Thus, it is reasonable to adopt the simplified signal model in (1) for further analysis. Also, we assume that the SS and SD are unaware of the existence of the legitimate monitor, and thus, do not employ any anti-eavesdropping or anti-jamming methods [29]. As defined in [11], [13], the instantaneous capacity of SS-LM link is known as monitoring rate, written as

$$R_{SM} = \log_2(1 + \gamma_s |\mathbf{h}_{RM}^H \Theta \mathbf{h}_{SR}|^2), \quad (3)$$

while the instantaneous capacity of the SS-SD link is referred to as suspicious rate, given by

$$R_{SD,n} = \log_2 \left(1 + \frac{\gamma_s |h_{SD} + \mathbf{h}_{RD}^H \Theta \mathbf{h}_{SR}|^2}{\gamma_J |\mathbf{h}_{RD}^H \Theta \mathbf{h}_{nR}|^2 + 1} \right), \quad (4)$$

where $\gamma_s = P_s/N_0$ and $\gamma_J = P_J/N_0$.

B. Surveillance Success Probability

In this section, we introduce the performance metric for physical-layer surveillance. As discussed in Section I, the relative monitoring rate (RMR) is defined as the difference between the monitoring rate and the suspicious rate, which is mathematically expressed as [30]

$$R_{M,n} = [R_{SM} - R_{SD,n}]^+, \quad (5)$$

where $[x]^+ = \max\{0, x\}$. To define a successful monitoring event, we consider that the RMR must be higher than a threshold R_{th} , which represents the minimum target rate for the legitimate monitor to decode successfully. The probability of this event is known as surveillance success probability (SSP) and is given by

$$P_{ss} = \Pr(R_{M,n} > R_{th}), \quad (6)$$

where the criterion for choosing n is specified in the following section.

III. PROPOSED RIS-AIDED MONITORING SCHEMES AND SSP ANALYSIS

While monitoring schemes using full CSI knowledge could theoretically offer the best performance, they require an unlimited and unrealistic amount of feedback, which is not practically appealing. In this section, we propose RIS-aided monitoring schemes where the RIS phase shifts are optimized

¹Each node is assumed to have a single antenna, while multi-antenna nodes is left for future work.

based on partial CSI. Our approach not only lowers the complexity of phase shift optimization but also reduces the feedback overhead associated with CSI acquisition. From (5), it is straightforward to see that, to maximize R_M , we can increase R_{SM} and decrease R_{SD} . However, these two objectives are conflicting because R_{SM} and R_{SD} are interdependent due to their dependence on the same phase shifts of the RIS, which affects the CSI of both links. To address this,

if both the CSI of the LS link and the CJ link are known, we optimize the RIS phase shift to maximize R_{SM} and perform jammer selection to minimize R_{SD} . But if only the CSI of the CJ link is known, we both optimize the RIS phase shift and use jammer selection to minimize R_{SD} .

Based on this strategy, we respectively propose two RIS-aided monitoring schemes: RISLO and RISCO. In RISLO, the LM exploits the CSI of the LS link combined with an optimally selected jammer. On the other hand, in RISCO, the LM utilizes the CSI of the CJ link plus an optimally selected jammer scheme. In addition, we provide a closed-form analysis of the SSP for both schemes.

A. RISLO: RIS phase optimization based on Legitimate surveillance channel with Optimal jammer selection

1) *Phase optimization and jammer selection:* To maximize R_{SM} given by (3) in the RISLO scheme, the phase shifts are designed to improve the average gain of SS-LM transmission, which are given by

$$\phi_l^{\text{RISLO}} = \arg(h_{R_{iM}}^* + \arg(h_{SR_l})), \quad \forall l \in \mathcal{L}. \quad (7)$$

Also, in the RISLO scheme, we opportunistically choose the jammer whose channel helps to reduce R_{SD} . By referring to (4), we select the optimal jammer as

$$n^{\text{RISLO}} = \arg \max_{n \in \mathcal{N}} Y_{1,n}^{\text{RISLO}}, \quad (8)$$

where $Y_{1,n}^{\text{RISLO}} = |\mathbf{h}_{RD}^H \Theta^{\text{RISLO}} \mathbf{h}_{nR}|^2$ denotes the CSI of RIS-aided CJ channels, whose maximization leads to a degradation of R_{SD} .

2) *SSP Analysis of RISLO:* By adopting the proposed RISLO scheme, (4) can be rewritten as

$$R_{SD}^{\text{RISLO}} = \log_2 \left(1 + \frac{\gamma_s Y_2}{\gamma_J \max_{n \in \mathcal{N}} Y_{1,n}^{\text{RISLO}} + 1} \right), \quad (9)$$

where $Y_2 = |h_{SD} + \mathbf{h}_{RD}^H \Theta^{\text{RISLO}} \mathbf{h}_{SR}|^2$ is the cascaded channel gain of the suspicious link, wherein Θ^{RISLO} denotes the phase shift design of RIS. To start with, we derive the necessary statistical distributions to facilitate subsequent derivations. In the RISLO scheme, Θ^{RISLO} , with regard to the LS link given by (7),

observes equivalent features as random phase shifts in Y_2 and $Y_{1,n}^{\text{RISLO}}$ (see Appendix) owing to the independence of the LS link and CJ links. From the Appendix, Y_2 and $Y_{1,n}^{\text{RISLO}}$ follow exponential distributions. Considering $Y_{1,n}^{\text{RISLO}}$ is independently-not-necessarily-identically-distributed, its CDF can be given by

$$F_{Y_{1,n}^{\text{RISLO}}}(y) = 1 - e^{-\frac{L\sigma_{nR}^2\sigma_{RD}^2}{y}}. \quad (10)$$

Besides, Y_2 follows an exponential distribution given by (38). By letting $W = |\mathbf{h}_{RM}^H \Theta^{\text{RISLO}} \mathbf{h}_{SR}|$ and using (7), W is simplified to

$$W = \sum_{l=1}^L |h_{R_{iM}}| |h_{SR_l}|, \quad (11)$$

where $h_{R_{iM}}$ and h_{SR_l} are modeled as independent zero-mean complex Gaussian random variables with respective variances of σ_{RM}^2 and σ_{SR}^2 , by considering independently and identically distributed Rayleigh fading channels from different reflecting elements of a RIS. By exploiting the Laguerre series approximation and by following the literatures on RISs [32][33], we approximate the cumulative density function (CDF) of W_1 as a Gamma distribution given by

$$\Pr(W \leq w) = 1 - \frac{\Gamma(\lambda, \frac{w}{w_1})}{\Gamma(\lambda)}, \quad (12)$$

with shape and scale parameters given as

$$\lambda = \frac{E^2(W)}{\text{Var}(W)} = \frac{\pi^2 L}{16 - \pi^2}, \quad w_1 = \frac{\text{Var}(W)}{E(W)}. \quad (13)$$

where $E(W)$ and $\text{Var}(W)$ denotes the mean and variance of W , respectively. The method above is named moment-match, which works well for positive random variables whose PDF has a single maximum and fast decaying tails [31]. To figure the statistical parameters, we derive

$$E(W) = \frac{\pi L}{16} \sigma_{RM} \sigma_{SR}, \quad (14)$$

and

$$\begin{aligned} \text{Var}(W) &= \pi L [E(|h_{RM}|^2 |h_{SR}|^2) - E^2(|h_{RM}| |h_{SR}|)] \\ &= \pi L \sigma_{RM}^2 \sigma_{SR}^2 \left(1 - \frac{\pi^2}{16}\right), \end{aligned} \quad (15)$$

where 11-(15) completes the statistical characterization of channel gain from LS link.

Letting $V = \frac{2^{R_{th}} Y_2}{\gamma_J \max_{n \in \mathcal{N}} Y_{1,n}^{\text{RISLO}} + 1}$, we obtain the CDF of V as

$$\begin{aligned} F_V(v) &= \Pr(V \leq v) \\ &= \int_0^\infty \frac{1}{\Xi} e^{-\frac{y}{\Xi}} \left[1 - \prod_{n \in \mathcal{N}} \left(1 - e^{-\frac{2^{R_{th}} y - 1}{v(L\sigma_{nR}^2\sigma_{RD}^2)}} \right) \right] dy \\ &= \int_0^\infty \frac{e^{-\frac{1}{v(L\sigma_{nR}^2\sigma_{RD}^2)}}}{\Xi} e^{-\frac{y}{\Xi}} \sum_{t=1}^{2^N-1} (-1)^{|J_t|+1} e^{-\sum_{J_t} \frac{y}{v(L\sigma_{nR}^2\sigma_{RD}^2)}} dy \\ &= \sum_{n=1}^N \binom{N}{n} \frac{(-1)^{n+1} v e^{-\frac{1}{v(L\sigma_{nR}^2\sigma_{RD}^2)}}}{v + n\delta_1}, \end{aligned} \quad (16)$$

where the binomial expansion theorem is used, and the CSI for N different jammers is considered independent. J_t represents the t -th non-empty subcollection of the jammer set \mathcal{N} , and $\delta_1 = \frac{2^{R_{th}} \Xi}{\gamma_J (L\sigma_{nR}^2\sigma_{RD}^2)}$. Besides, $|J_t|$ denotes the cardinality of the set J_t , and $\binom{N}{n}$ is the number of all possible subcollections satisfying $|J_t| = n$. By substituting (12) and (16) into (9), the SSP of the RISLO scheme can be derived as

$$\begin{aligned} P_{ss}^{\text{RISLO}} &= \Pr(R_{SM} - R_{SD}^{\text{RISLO}} > R_{th}) \\ &= \int_0^\infty \frac{f_{W_1}(\sqrt{v+\beta})}{2\sqrt{v+\beta}} F_V(v) e^{-\frac{1}{v(L\sigma_{nR}^2\sigma_{RD}^2)}} dv. \end{aligned} \quad (17)$$

Substituting (16) into (17), and capitalizing on the Gaussian-Chebyshev quadrature [36], the SSP of the RISLO scheme is given by (18) at the top of next page, where $\theta_k = \cos\left(\frac{2k-1}{2K}\pi\right)$, $\tau_k = \frac{(\theta_k+1)\pi}{4}$, and K is accuracy versus complexity parameter.

To highlight the performance gain from jammer selection, we adopt the RISLR as a benchmark scheme corresponding to RISLO. The RISLR adopts an equal-probability selection from the set \mathcal{N} instead of (8). The SSP expression of RISLR is written as 19 at the top of next page as for a comparison, but the derivation is the same as that in this section and is omitted.

Remark 1: When P_j approaches to infinity, we know δ_1 becomes very small and even close to 0. By comparing (18) and 19, given $\sum_{n=0}^N \binom{N}{n} (-1)^n = 0$, then the two expressions are close to a same value when $\delta_1 \rightarrow 0$. This tells us that the benefit of CSI-based jammer selection is marginal because all transmissions of CJ links are in pretty good quality. By contrast, when the jamming power decreases, δ_1 becomes larger, then the RISLO behaves significantly different from RISLR.

B. RISCO: RIS phase optimization based on Cooperative jamming channel with Optimal jammer selection

1) *Phase optimization and jammer selection:* The RISCO scheme refers to the case that the RIS phase shifts are considered according to the CSI of CJ links. Although $Y_{1,n} = |\mathbf{h}_{\text{RD}}^H \Theta \mathbf{h}_{\text{NR}}|^2$ shows a dependence on the varying channel quality for $n \in \mathcal{N}$, we optimize the phase shift for maximizing $Y_{1,n}$ when given the jammer n is chosen. Then, the desired phase shifts aim at maximizing the average gain of channels from the monitor to the suspicious receiver, given by

$$\phi_{l,n}^{\text{RISCO}} = \arg(h_{\text{RD}}^*) + \arg(h_{nR_l}), \quad \forall l \in \mathcal{L}. \quad (20)$$

Substituting (20) into $Y_{1,n}$, the maximized channel gain is denoted as

$$Y_{1,n}^{\text{RISCO}} = \sum_{l=1}^L |h_{\text{RD}}| |h_{nR_l}|. \quad (21)$$

Meanwhile, the RISCO is also assisted by jammer selection with the CSI of LM-SD transmissions. In the RISCO scheme, likewise as (8), we select the optimal jammer to decrease R_{SD} as

$$n^{\text{RISCO}} = \arg \max_{n \in \mathcal{N}} Y_{1,n}^{\text{RISCO}}. \quad (22)$$

2) *SSP Analysis of RISCO:* It can be seen from (20) that Θ^{RISCO} is designed as

$$\Theta^{\text{RISCO}} = \text{diag}(e^{-j[\arg(\mathbf{h}_{\text{RD}}^H) + \arg(\mathbf{h}_{n^{\text{RISCO}}})]}),$$

where n^{RISCO} is given by (22). Different from $Y_{1,n}^{\text{RISLO}}$, then, $Y_{1,n}^{\text{RISCO}}$ is characterized analogously as W , and the derivation is omitted. From (12), the CDF of $Y_{1,n}^{\text{RISCO}}$ can be given by

$$\Pr(Y_{1,n}^{\text{RISCO}} \leq w) = 1 - \frac{\Gamma(\lambda_2, \frac{w}{w_{2,n}})}{\Gamma(\lambda_2)}, \quad (23)$$

where

$$\lambda_2 = \frac{\pi^2 L}{16 - \pi^2} = \lambda, \quad (24)$$

wherein λ is also given in (13) and

$$w_{2,n} = \frac{(16 - \pi^2) \sigma_{\text{RD}} \sigma_{\text{NR}}}{4\pi}. \quad (25)$$

Similar as proof in Appendix A, the phase shift of RIS given by (20) is random for the LS link. Then, $Y_2 = |h_{\text{SD}} + \mathbf{h}_{\text{RD}}^H \Theta^{\text{RISCO}} \mathbf{h}_{\text{SR}}|^2$ is the same as that of the RISLO scheme. By letting $Z_1 = |\mathbf{h}_{\text{RM}}^H \Theta^{\text{RISCO}} \mathbf{h}_{\text{SR}}|^2$, and Z_1 follows an exponential distribution with its CDF given by

$$F_{Z_1}(z) = 1 - e^{-\frac{z}{L\sigma_{\text{SR}}^2\sigma_{\text{RM}}^2}}. \quad (26)$$

Letting $G = \frac{Y_2}{Z_1 - \beta}$, where $\beta = \frac{2^{R_{\text{th}}}-1}{\gamma_s}$, we derive the CDF of G as

$$\begin{aligned} F_G(g) &= \int_0^\infty \frac{1}{\Xi} e^{-\frac{y}{\Xi}} e^{-\frac{y+\beta}{L\sigma_{\text{SR}}^2\sigma_{\text{RM}}^2}} dy \\ &= \frac{ge^{-\frac{\beta}{L\sigma_{\text{SR}}^2\sigma_{\text{RM}}^2}}}{g + \delta_2}, \end{aligned} \quad (27)$$

where $\delta_2 = \frac{\Xi}{L\sigma_{\text{SR}}^2\sigma_{\text{RM}}^2}$. Likewise as (9), we obtain the suspicious rate of the RISCO scheme as

$$R_{\text{SD}}^{\text{RISCO}} = \log_2 \left(1 + \frac{\gamma_s Y_2}{\gamma_j \max_{n \in \mathcal{N}} Y_{1,n}^{\text{RISCO}} + 1} \right). \quad (28)$$

By letting $T = \max_{n \in \mathcal{N}} Y_{1,n}^{\text{RISCO}}$, then the PDF of T can be obtained as (29) at the top of the page, where the generalized multinomial theorem is utilized, and $P_{q,n}$ represents the q -th non-empty subcollection of the jammer set $\{\mathcal{N} - n\}$, $|P_{q,n}|$ denote the cardinality of the set $P_{q,n}$. Besides, note that the set $\mathcal{S} = \{(n_1, n_2, \dots, n_\lambda) | \sum_{p=1}^\lambda n_p = |P_{q,n}|\}$, $A_1 = \frac{\prod_{k=1}^\lambda ((k-1)!)^{n_k}}{\prod_{p=1}^\lambda n_p!}$, $B_1 = \sum_{p=1}^\lambda n_p (p-1)$.

Then, the SSP of the RISCO scheme can be derived as

$$\begin{aligned} P_{\text{ss}}^{\text{RISCO}} &= \Pr(R_{\text{SM}} - R_{\text{SD}}^{\text{RISCO}} > R_{\text{th}}) \\ &= \int_{\frac{1}{\sqrt{\gamma_j}}}^\infty \frac{\sqrt{\gamma_j} f_T \left(\sqrt{\frac{\gamma_j g^2 - 1}{2^{R_{\text{th}}}}} \right)}{\sqrt{2^{R_{\text{th}}}}} F_G(g^2) dg. \end{aligned} \quad (30)$$

Substituting (27) and (29) into (30), the closed-form SSP expression of the RISCO scheme given by (31) at the top of next page, where $\beta = \frac{2^{R_{\text{th}}}-1}{\gamma_s}$, $G_{p,q}^{m,n}(\cdot)$ is the Meijer G-function [37, Eq. (9.301)], and the result of [37, Eq. (3.389-2)] is used.

IV. ASYMPTOTIC ANALYSIS IN USEFUL SPECIAL CASES

Since the intricate SSP expressions involving the special functions (e.g., Meijer G-function) are unable to provide performance comparison between different schemes, we present asymptotic analysis considering some limitations in practical applications, capturing more insights for decisions of system designers, e.g., which scheme to choose in a particular system. Several proposed schemes have shown obviously competitive performance exploiting proactive monitors, but it is not fair to compare with passive monitoring because of the extra power consumption and implementation complexity of full-duplex

$$P_{ss}^{\text{RISLO}} = \frac{\pi^2}{4K} \sum_{k=1}^K \sum_{n=1}^N \binom{N}{n} \frac{(-1)^{n+1} \sqrt{1-\theta_k^2} \sec^2 \tau_k \tan \tau_k (\sqrt{\tan \tau_k + \beta})^{\lambda-2} e^{-\frac{\sqrt{\tan \tau_k + \beta}}{w_1}} e^{\frac{1}{\tan \tau_k (L\sigma_{nR}^2 \sigma_{RD}^2)}}}{2w_1^\lambda (\lambda-1)! (\tan \tau_k + n\delta_1)}. \quad (18)$$

$$P_{ss}^{\text{RISLR}} = \frac{\pi^2}{4K} \sum_{k=1}^K \frac{\sqrt{1-\theta_k^2} \sec^2 \tau_k \tan \tau_k (\sqrt{\tan \tau_k + \beta})^{\lambda-2} e^{-\frac{\sqrt{\tan \tau_k + \beta}}{w_1}} e^{\frac{1}{\tan \tau_k (L\sigma_{nR}^2 \sigma_{RD}^2)}}}{2w_1^\lambda (\lambda-1)! (\tan \tau_k + \delta_1)}. \quad (19)$$

$$\begin{aligned} f_T(t) &= \sum_{n=1}^N \frac{t^{\lambda-1}}{(\mu_n)^\lambda (\lambda-1)!} e^{-\frac{t}{\mu_n}} \prod_{m \in \{N-n\}} \left(1 - e^{-\frac{t}{\mu_m}} \left(\sum_{k=1}^{\lambda-1} \frac{t^k}{\mu_m^k} \right) \right) \\ &= \sum_{n=1}^N \frac{1}{(\lambda-1)!} \left(1 + \sum_{q=1}^{2^{N-1}-1} (-1)^{|P_{q,n}|} \sum_{m \in P_{q,n}} e^{-\frac{t}{\mu_n} - \frac{|P_{q,n}|t}{\mu_m}} \sum_S \frac{A_1}{(\mu_m)^{B_1}} t^{B_1+\lambda-1} \right). \end{aligned} \quad (29)$$

$$P_{ss}^{\text{RISCO}} = \frac{e^{-\frac{\beta}{L\sigma_{SR}^2 \sigma_{RM}^2}}}{2\sqrt{\pi} (\lambda-1)!} \sum_{n=1}^N \frac{1}{(\mu_n)^\lambda} \left(1 + \sum_{q=1}^{2^{N-1}-1} \sum_{m \in P_{q,n}} \frac{(-1)^{|P_{q,n}|}}{|P_{q,n}|!} \sum_S A_1 \delta_2^{\frac{\lambda+B_1}{2}} G_{1,3}^{3,1} \left(\frac{(\mu_n + |P_{q,n}| \mu_m)^2 \delta_2}{4} \middle| \begin{matrix} -\frac{\lambda+B_1}{2} \\ -\frac{\lambda+B_1}{2}, 0, \frac{1}{2} \end{matrix} \right) \right). \quad (31)$$

devices. Besides, it is preferred to consider the monitor to be invisible to the suspicious pairs, where jamming power control should be focused as well. Otherwise, the suspicious receiver becomes aware and takes anti-jamming measures, causing all our jammers to suffer performance loss.

With $P_J \rightarrow 0$ to characterize a case where the jammers are nearly passive with low transmit power, the derived expression is simplified, making it evident to provide some findings. Then, (9) can be reduced to

$$R_{SD}^{\text{RISLO,Pas}} = \log_2(1 + \gamma_s Y_2), \quad (32)$$

where the ‘‘Pas’’ is a short hand for $P_J \rightarrow 0$, meaning the low jamming SNR which is approximated as passive monitoring. Also, focusing on the monitoring performance bound, we set $R_{th} = 0$, which does not change the trend of SSP functions. By combining (18) and (32), the asymptotic SSP of the RISLO scheme can be expressed as

$$\begin{aligned} P_{ss}^{\text{RISLO,Pas}} &= \Pr(W_1^2 > Y_2) \\ &= \left(\frac{4w_1^2}{L\sigma_{nR}^2 \sigma_{RD}^2} \right)^{\frac{1}{4} - \frac{\lambda}{2}} e^{\frac{L\sigma_{nR}^2 \sigma_{RD}^2}{8w_1^2}} \mathcal{W}_{\frac{1}{4} - \frac{\lambda}{2}, -\frac{1}{4}} \left(\frac{L\sigma_{nR}^2 \sigma_{RD}^2}{4w_1^2} \right), \end{aligned} \quad (33)$$

where $\mathcal{W}_{a,b}(\cdot)$ is the Whittaker function defined as [37, Eq. (9.222-2)], and the result of [37, Eq. (3.462-1)] and the definition of parabolic cylinder functions [37, Eq. (9.240)] are used. It is still challenging to gain more insights from the complex expression containing the Whittaker function. To highlight the performance gains brought by the RIS, we consider the case of asymptotically large number of RIS elements, i.e., $L \rightarrow \infty$. With $\frac{L\sigma_{nR}^2 \sigma_{RD}^2}{4w_1^2}$ in 33 approaching infinity, the Whittaker function can be expanded according to Watson’s lemma [37], expressed as

$$W_{a,b}(z) \sim e^{-\frac{z}{2}} z^a \sum_{m=0}^{\infty} \frac{(-1)^m \left(\frac{1}{2} - a + b\right)_m \left(\frac{1}{2} - a - b\right)_m}{n! z^m}, \quad (34)$$

where $(a_p)_k = \frac{\Gamma(a_p+k)}{\Gamma(a_p)}$, $a = \frac{1}{4} - \frac{\lambda}{2}$ and $b = -\frac{1}{4}$, also $z = \frac{L\sigma_{nR}^2 \sigma_{RD}^2}{4w_1^2}$. Then, 33 can be converted to

$$\begin{aligned} P_{ss}^{\text{RISLO,Pas}} &= \sum_{m=0}^{\infty} \frac{(-1)^m \left(\frac{1}{2} - a + b\right)_m \left(\frac{1}{2} - a - b\right)_m}{n! z^m} \\ &\stackrel{(a)}{=} \mathcal{O}(e^{-\frac{1}{z}}), \end{aligned} \quad (35)$$

where the equality of (a) holds utilizing the Taylor expansion, and $\mathcal{O}(e^{-\frac{1}{z}})$ means a similar asymptotic behavior as $e^{-\frac{1}{z}}$ given $L \rightarrow \infty$, i.e., $z \rightarrow \infty$.

By combining (18) and (32), also by using (10) and (26), the asymptotic SSP of the RM-CSICJ framework can be expressed as

$$\begin{aligned} P_{ss}^{\text{RISCO,Pas}} &= \Pr(Z_1 > Y_2) \\ &= \frac{1}{1 + \delta_2}, \end{aligned} \quad (36)$$

where $\delta_2 = \frac{\sigma_{SD}^2 + L\sigma_{RD}^2 \sigma_{SR}^2}{L\sigma_{SR}^2 \sigma_{RM}^2}$.

Remark 2: The performance gain brought by the RIS can be revealed by a comparative analysis of 33 and 36. It can be seen that with an asymptotically large number of RIS elements, the performance ceilings of the RISLO and RISCO schemes are surprisingly different. When L becomes sufficiently large, P_{ss}^{RISLO} approaches to one in an exponential speed. In contrast, although $P_{ss}^{\text{RISCO,Pas}}$ can also be proved as an increasing function of L , it only converges to a constant between zero and one. Specifically, for notation convenience, we define the ratio of average gains between the monitoring channel and suspicious channel, referred to as the monitoring to suspicious ratio (MSR) and denoted as $\zeta_{MSR} = \frac{\sigma_{SR}^2}{\sigma_{n2}^2}$ where $n1 \in \{RM, nR\}$ and $n2 \in \{SR, RD\}$, indicating a channel quality comparison between suspicious links and monitoring links. Then, with $L \rightarrow \infty$, $\delta_2 \rightarrow \frac{1}{\zeta_{MSR}}$, i.e., $P_{ss}^{\text{RM-CSICJ,Pas}} \rightarrow \frac{\zeta_{MSR}}{\zeta_{MSR}+1}$. This tells that only when the LS and CJ links are much better than the suspicious links, the RISCO scheme exploits a theoretically

good performance bound, but it is not guaranteed in the system.

V. SIMULATION RESULTS AND DISCUSSIONS

In this section, we present some simulation results. The numerical values of parameters are listed in Table I on top of the page, unless otherwise stated. Besides, σ_{nR}^2 are specified as the same value for $n \in \mathcal{N}$ without loss of generality. It is worth mentioning that in Fig. 2-Fig. 6, theoretical expressions given by (18), 19, and (31) are described as lines and Monte-Carlo simulations are plotted as dotted markers, whose well matches verify the correctness of closed-form analysis. Indeed, the obtained expressions provide an alternative to time-consuming simulations for evaluating system monitoring performance.

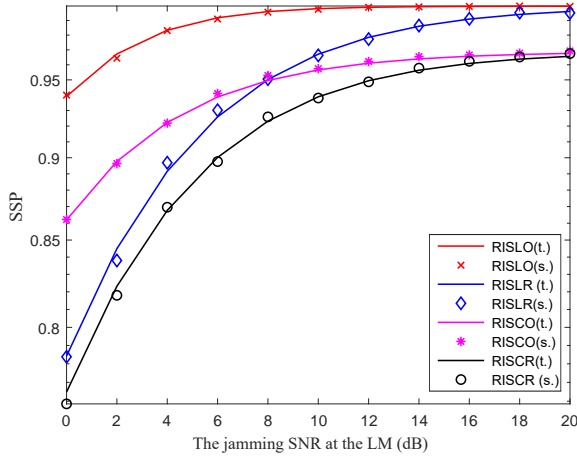


Fig. 2. Surveillance outage probability of RISLR, RISLO, RISCRC, and RISCO schemes versus jamming SNR, where “t.” and “s.” stand for theoretical and simulation results, respectively.

Fig. 2 plots the surveillance success probabilities (SSPs) of RISLR, RISLO, RISCRC, and RISCO schemes versus jamming SNR. With a growing jamming SNR, the SSPs of all schemes increase. In the low jamming SNR region, the SSPs of jammer-selected schemes generally exploit higher SSPs, due to the fact that the channel gains of CJ links become essential when the jammers are power-constrained. This can also be proved by the analytical results in Section IV. Conversely, in the high jamming SNR region, the RISLO outperform the RISCO scheme in terms of SSPs, which gradually converge towards their respective performance ceiling, similar to what mentioned in remark 2. The difference between ceilings of two schemes showing a remarkable advantage of RISLO over RISCO. This is because that the CSI database of the RISLO for phase shift design and jammer selection includes both knowledges of LS and CJ links, while the RISCO only knows the CSI of CJ links. Thus, the RISLO exploits CSI better than the RISCO.

Fig. 3 depicts the SSPs of RISLR, RISLO, RISCRC, and RISCO schemes versus monitoring to suspicious ratio (MSR). The low MSR region refers to the situation that the channel gains of suspicious links are large compared to that of the monitoring links, and vice versa. Specifically, the MSR below zero means the monitoring channels are worse than the suspicious

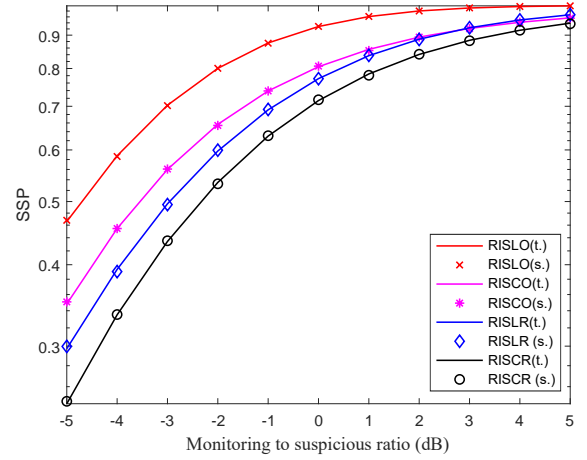


Fig. 3. Surveillance success probability of RISLR, RISLO, RISCRC, and RISCO schemes versus MSR.

channels. As can be observed, with the same jammer selection strategy, the SSP of the RISLO scheme is significantly higher than that of the RISCO. Moreover, schemes with an optimally selected jammer show a better SSP performance at the cost of gaining CSI knowledge, especially in the low MSR region.

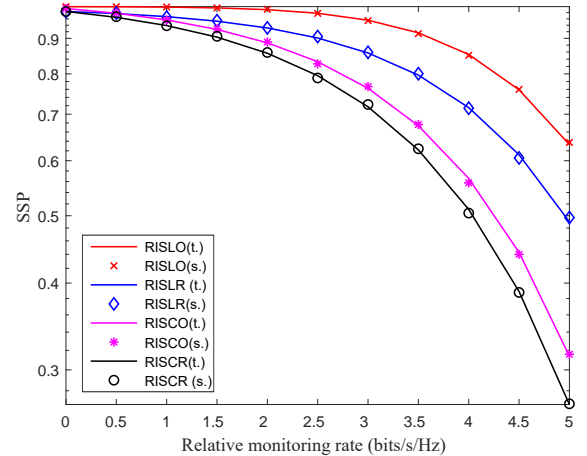


Fig. 4. Surveillance success probability of RISLR, RISLO, RISCRC, and RISCO schemes versus relative monitoring rate.

Fig. 4 shows the SSPs of RISLR, RISLO, RISCRC, and RISCO schemes versus RMR, which is a target for the reliability of monitoring. It can be known that the OJS schemes always witness an obviously better performance than conventional RIS schemes. Furthermore, it is found that the performance gap between the RISLO and RISCO schemes become more obvious as the target RMR grows larger.

Fig. 5 shows the SSPs of RISLR, RISLO, RISCRC, and RISCO schemes versus transmit SNR at the SS. Although the SSPs of all schemes rise when transmit power of suspicious communication increases, this may not happen when the illegal party intend to make covert communication quietly. Usually, if the illegal party want the message only to be known by suspicious nodes, they will limit transmit power to avoid being detected. Henceforth, with a low SNR at the SS, the jammer

TABLE I
SIMULATION PARAMETERS

Descriptions	Symbols	Values
The variances of reflection channel coefficients	$\sigma_{rR}^2, \sigma_{RM_1}^2, \sigma_{SR}^2, \sigma_{RD}^2$	0.5
The variances of direct (non-RIS) channel coefficients	σ_{SD}^2	1
Transmit SNR at the SS	γ_s	10dB
Jamming SNR	γ_j	10dB
MSR	ζ_{MSR}	5dB
The number of jammers	N	3
The number of RIS reflecting elements	L	4
Relative monitoring rate	R_{th}	1bit/s/Hz
The accuracy versus complexity parameter in the sum approximation	K	400

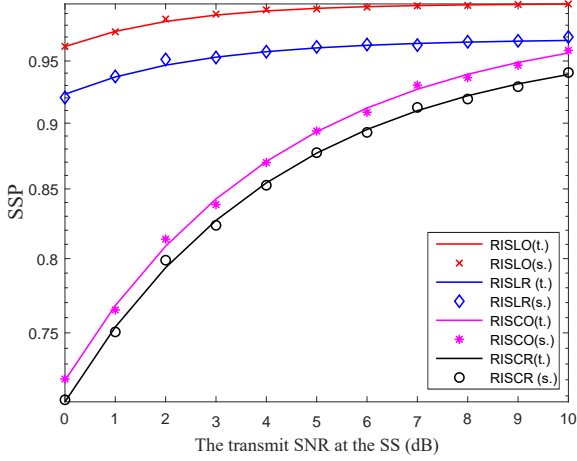


Fig. 5. Surveillance success probability of RISLR, RISLO, RISCR, and RISCO schemes versus the transmit SNR at the SS.

selected schemes improve SSP greatly compared to the non-jammer-selection ones.

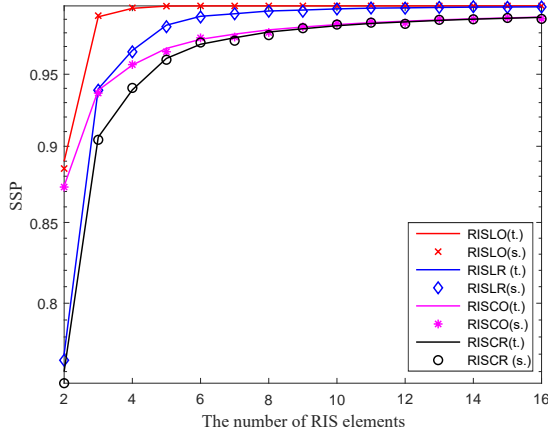


Fig. 6. Surveillance success probability of RISLR, RISLO, RISCR, and RISCO schemes versus the number of RIS elements.

From Fig. 6, we observe the SSPs of RISLR, RISLO, RISCR, and RISCO schemes versus the number of RIS elements in the suspicious link. With an increasing number of RIS elements, the SSPs of all schemes increase rapidly. When the number of RIS elements is small, the jammer selected schemes are generally superior to the non-jammer-selection ones. With an increasing number of RIS elements, one can observe from

Fig. 6 that the RISLO(R) and RISCO(R) converges to different performance ceilings as suggested by remark 2, showing their system performance gain assisted by a RIS. This result again prove that CSI acquisition and phase shift accuracy can be a cornerstone of RIS-aided communications.

VI. CONCLUSION

In this paper, we presented a RIS-aided wireless surveillance system assisted by multiple jammers. We proposed RISLO and RISCO schemes which jammer selection strategies are separately incorporated. We derived the SSP expressions and revealed a tradeoff between monitoring performance and jammer implementation complexity, where CSI utilization played a leading role. Simulation results not only confirmed our closed-form analysis, but also demonstrated the advantage of jammer selection strategy.

APPENDIX

We firstly prove the phase shifts of RIS to maximize the average gain of LS link is random from the perspective of CJ link. This “random” means a uniform distribution on the range $[0, 2\pi)$. From(20), the phase shifts are extracted from the phase angles of h_{R_lM} and h_{SR_l} ($l \in \mathcal{L}$) for L reflecting links, which are complex Gaussian random variables. Then the phase shifts follow a uniform distribution on the range $[0, 2\pi)$. Utilizing the independence of suspicious links and monitoring links, the phase shifts are completely random for other links [35]. The next step is to figure out the distribution of Y_2 (as an example) with random phase shifts. Since Y_2 can be expanded as

$$\mathbf{h}_{RM} \Theta \mathbf{h}_{SR} = \underbrace{\sum_{l=1}^L |h_{R_lM}| |h_{SR_l}| \cos(\phi_{R_lM} + \phi_{SR_l} + \phi_l)}_{X_1} + j \underbrace{\sum_{l=1}^L |h_{R_lM}| |h_{SR_l}| \sin(\phi_{R_lM} + \phi_{SR_l} + \phi_l)}_{X_2}, \quad (37)$$

where $l \in \mathcal{L}$, and j is the imaginary unit. In 37, ϕ_l given by(20) is a uniformly-distributed variable independent from ϕ_{R_lD} and ϕ_{SR_l} . Using the periodicity of trigonometric functions \cos and \sin , for $\varphi \in [0, 2\pi)$ randomly, $E(\cos \varphi) = E(\sin \varphi) = 0$ and $E(\cos^2 \varphi) = E(\sin^2 \varphi) = \frac{1}{2}$. Exploiting the central limit theorem for large number of reflecting elements [34], we know that $X_1 \sim \mathcal{CN}(0, \frac{\sigma_{SD}^2}{2} + \frac{L\sigma_{RD}^2\sigma_{SR}^2}{2})$, $X_2 \sim \mathcal{CN}(0, \frac{\sigma_{SD}^2}{2} + \frac{L\sigma_{RD}^2\sigma_{SR}^2}{2})$.

Given $Y_2 = X_1 + jX_2$, we prove that Y_2 follows a Rayleigh distribution given by

$$F_{Y_2}(y) = 1 - e^{-\frac{y}{\sigma_{SD}^2 + L\sigma_{RD}^2\sigma_{SR}^2}}. \quad (38)$$

Furthermore, to obtain more intuitive proof for an exponentially distributed variable related to channel gains, we present numerical results below to verify the accuracy of this formulation. As shown from Fig. 7, on the one hand, the cascaded links where RIS phase shifts aligning with CSI of other links are plotted as lines. On the other hand, the cascaded links with random RIS phase shifts are plotted as dotted markers. Throughout different statistical parameters, the close agreements prove that the phase shifts to maximize the average gain of SS-LM transmission is random from the perspective of LM-SD transmission.

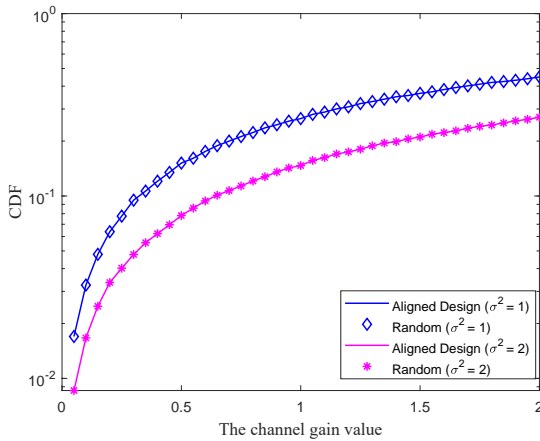


Fig. 7. The comparison between different generations of the RIS phase shifts to validate the random assumption.

REFERENCES

- [1] Y. Zou, J. Zhu, X. Wang, and L. Hanzo, "A Survey on wireless security: Technical challenges, recent advances, and future trends," *Proc. IEEE*, vol. 104, no. 9, pp. 1727–1765, Sep. 2016.
- [2] P. Yan, W. Duan, Q. Sun, G. Zhang, J. Zhang, and P.-H. Ho, "Improving physical-layer security for cognitive networks via artificial noise-aided rate splitting," *IEEE Internet of Things J.*, to appear, doi: 10.1109/JIOT.2024.3367889.
- [3] H. Lei, C. Gao, I. S. Ansari, Y. Guo, G. Pan, and K. A. Qaraqe, "On physical-layer security over SIMO generalized-K fading channels," *IEEE Trans. Veh. Tech.*, vol. 65, no. 9, pp. 7780–7785, Sep. 2016.
- [4] J. Xu, L. Duan, and R. Zhang, "Surveillance and intervention of infrastructure-free mobile communications: A new wireless security paradigm," *IEEE Wireless Commun.*, vol. 24, no. 4, pp. 152–159, Aug. 2017.
- [5] Terrorist Surveillance Program [Online] Available: https://en.wikipedia.org/wiki/Terrorist_Surveillance_Program.
- [6] J. Xu, L. Duan, and R. Zhang, "Proactive eavesdropping via jamming for rate maximization over Rayleigh fading channels," *IEEE Wireless Commun. Lett.*, vol. 5, no. 1, pp. 80–83, Feb. 2016.
- [7] Z. Cheng et al., "Covert surveillance via proactive eavesdropping under channel uncertainty," *IEEE Trans. Commun.*, vol. 69, no. 6, pp. 4024–4037, Jun. 2021.
- [8] J. Moon, H. Lee, C. Song, S. Kang, and I. Lee, "Relay-assisted proactive eavesdropping with cooperative jamming and spoofing," *IEEE Trans. Wireless Commun.*, vol. 17, no. 10, pp. 6958–6971, Oct. 2018.
- [9] Y. Zou, "Physical layer security for spectrum sharing systems," *IEEE Trans. Wireless Commun.*, vol. 16, no. 2, pp. 1319–1329, Feb. 2017.

- [10] Y. Sun et al., "RIS-assisted robust hybrid beamforming against simultaneous jamming and eavesdropping attacks," *IEEE Trans. Wireless Commun.*, vol. 21, no. 11, pp. 9212–9231, Nov. 2022.
- [11] S. Lin, Y. Zou, B. Li, and T. Wu, "Security-reliability tradeoff analysis of RIS-aided multiuser communications," *IEEE Trans. Veh. Tech.*, vol. 72, no. 5, pp. 6225–6237, May 2023.
- [12] J. Xu, L. Duan, and R. Zhang, "Proactive eavesdropping via cognitive jamming in fading channels," *IEEE Trans. Wireless Commun.*, vol. 16, no. 5, pp. 2790–2806, May 2017.
- [13] H. Xu and L. Sun, "Wireless surveillance via proactive eavesdropping and rotated jamming," *IEEE Trans. Veh. Tech.*, vol. 68, no. 11, pp. 10713–10727, Nov. 2019.
- [14] L. Sun, Y. Zhang, and A. L. Swindlehurst, "Alternate-jamming-aided wireless physical-layer surveillance: Protocol design and performance analysis," *IEEE Trans. Inf. Forensic Secur.*, vol. 16, pp. 1989–2003, 2021.
- [15] G. Hu, J. Ouyang, Y. Cai, and Y. Cai, "Proactive eavesdropping in two-way amplify-and-forward relay networks," *IEEE Syst. J.*, vol. 15, no. 3, pp. 3415–3426, Sep. 2021.
- [16] G. Hu, J. Si, Y. Cai, and N. Al-Dhahir, "Intelligent reflecting surface assisted proactive eavesdropping over suspicious broadcasting communication with statistical CSI," *IEEE Trans. Veh. Tech.*, vol. 71, no. 4, pp. 4483–4488, Apr. 2022.
- [17] C. Zhong, X. Jiang, F. Qu and Z. Zhang, "Multi-antenna wireless legitimate surveillance systems: Design and performance analysis," *IEEE Trans. Wireless Commun.*, vol. 16, no. 7, pp. 4585–4599, Jul. 2017.
- [18] D. Xu and H. Zhu, "Proactive eavesdropping of physical layer security aided suspicious communications in fading channels," *IEEE Trans. Inf. Forensic Secur.*, vol. 18, pp. 1111–1126, 2023.
- [19] Z. Zhu, C. Li, Y. Huang and L. Yang, "Non-outage probability of jamming-assisted continuous eavesdropping with multi-antenna," *IEEE Commun. Lett.*, vol. 26, no. 6, pp. 1236–1239, Jun. 2022.
- [20] D. Xu, "Legitimate surveillance with battery-aided wireless powered full-duplex monitor," *IEEE Syst. J.*, vol. 14, no. 4, pp. 5229–5232, Dec. 2020.
- [21] D. Xu and H. Zhu, "Proactive eavesdropping over multiple suspicious communication links with heterogeneous services," *IEEE Trans. Wireless Commun.*, 2022, doi: 10.1109/TWC.2022.3218553.
- [22] G. Hu, Y. Cai, and J. Ouyang, "Proactive eavesdropping via jamming for multichannel decode-and-forward relay system," *IEEE Commun. Lett.*, vol. 24, no. 3, pp. 491–495, Mar. 2020.
- [23] G. Hu et al., "Analysis and optimization of STAR-RIS-assisted proactive eavesdropping with statistical CSI," *IEEE Trans. Veh. Tech.*, doi: 10.1109/TVT.2022.3232990.
- [24] T. Ji, M. Hua, C. Li, Y. Huang, and L. Yang, "A robust IRS-aided wireless information surveillance design with bounded channel errors," *IEEE Wireless Commun. Lett.*, vol. 11, no. 10, pp. 2210–2214, Oct. 2022.
- [25] M. -M. Zhao, Y. Cai, and R. Zhang, "Intelligent reflecting surface aided wireless information surveillance," *IEEE Trans. Wireless Commun.*, vol. 22, no. 2, pp. 1219–1234, Feb. 2023.
- [26] Y. Li, H. Guo, Y. Chen, B. Lyu, and Y. Feng, "Reflect beamforming optimization for reconfigurable intelligent surface assisted cooperative jamming," *IEEE Commun. Lett.*, vol. 26, no. 9, pp. 2126–2130, Sep. 2022.
- [27] I. S. Gradshteyn and I. M. Ryzhik, *Table of Integrals, Series, and Products*, 6th ed. San Diego, CA, USA: Academic Press, 2000.
- [28] G. Hu, J. Si, and Z. Li, "Borrowing arrows with thatched boats: Exploiting the reactive primary communications for boosting jamming-assisted proactive eavesdropping," *IEEE Trans. on Mobile Computing*, doi: 10.1109/TMC.2022.3175357.
- [29] H. Zhang, L. Duan, and R. Zhang, "Jamming-assisted proactive eavesdropping over two suspicious communication links," *IEEE Trans. Wireless Commun.*, vol. 19, no. 7, pp. 4817–4830, Jul. 2020.
- [30] Z. Mobini, H. Q. Ngo, M. Matthaiou and L. Hanzo, "Cell-Free Massive MIMO Surveillance of Multiple Untrusted Communication Links," *IEEE Internet of Things Journal*, vol. 11, no. 20, pp. 33010–33026, 15 Oct. 15, 2024
- [31] S. Primak, V. Kontorovich, and V. Lyandres, "Stochastic methods and their applications to communications: Stochastic differential equations approach," *John Wiley Sons*, 2004.
- [32] Z. Sun and Y. Jing, "On the performance of multi-antenna IRS-assisted NOMA networks with continuous and discrete IRS phase shifting," *IEEE Trans. Wireless Commun.*, vol. 21, no. 5, pp. 3012–3023, May 2022.
- [33] Q. Li, M. El-Hajjar, I. Hemadeh, D. Jagyasi, A. Shojaeifard, and L. Hanzo, "Performance analysis of active RIS-aided systems in the face of imperfect CSI and phase shift noise," *IEEE Trans. Veh. Tech.*, early access, doi: 10.1109/TVT.2023.3239398, Jan. 2023.

- [34] C. Psomas and I. Krikidis, “Low-complexity random rotation-based schemes for intelligent reflecting surfaces,” *IEEE Trans. Wireless Commun.*, vol. 20, no. 8, pp. 5212-5225, Aug. 2021.
- [35] L. Lv, Q. Wu, Z. Li, Z. Ding, N. Al-Dhahir, and J. Chen, “Covert communication in intelligent reflecting surface-assisted NOMA systems: Design, analysis, and optimization,” *IEEE Trans. Wireless Commun.*, vol. 21, no. 3, pp. 1735-1750, Mar. 2022.
- [36] R. Janaswamy, “Consistency requirements for integral representations of green’s functions—Part II: An erroneous representation,” *IEEE Trans. on Antennas and Propag.*, vol. 66, no. 8, pp. 4069-4076, Aug. 2018.
- [37] F. W. Olver, D. W. Lozier, R. F. Boisvert, and W. C. Charles, *NIST handbook of mathematical functions*. Cambridge University Press, 2010.